INFECTION AND IMMUNITY, July 2007, p. 3581–3593 Vol. 75, No. 7
0019-9567/07/$08.00+0 doi:10.1128/IAI.00214-07

Adapter Protein SH2-Bβ Stimulates Actin-Based Motility of *Listeria monocytogenes* in a Vasodilator-Stimulated Phosphoprotein (VASP)-Dependent Fashion▽

Maria Diakonova,[1]†* Emmanuele Helfer,[3]† Stephanie Seveau,[2]‡ Joel A. Swanson,[2] Christine Kocks,[4] Liangyou Rui,[1] Marie-France Carlier,[3] and Christin Carter-Su[1]

Departments of Molecular and Integrative Physiology[1] and Microbiology and Immunology,[2] University of Michigan Medical School, Ann Arbor, Michigan; Dynamique du Cytosquelette Laboratoire d'Enzymologie et Biochimie Structurales, CNRS, Gif-sur-Yvette, France[3]; and Massachusetts General Hospital, Harvard Medical School, Boston, Massachusetts[4]

Received 8 February 2007/Returned for modification 20 March 2007/Accepted 10 April 2007

SH2-Bβ (Src homology 2 Bβ) is an adapter protein that is required for maximal growth hormone-dependent actin reorganization in membrane ruffling and cell motility. Here we show that SH2-Bβ is also required for maximal actin-based motility of *Listeria monocytogenes*. SH2-Bβ localizes to *Listeria*-induced actin tails and increases the rate of bacterial propulsion in infected cells and in cell extracts. Furthermore, *Listeria* motility is decreased in mouse embryo fibroblasts from SH2-B$^{-/-}$ mice. Both recruitment of SH2-Bβ to *Listeria* and SH2-Bβ stimulation of actin-based propulsion require the vasodilator-stimulated phosphoprotein (VASP), which binds ActA at the surfaces of *Listeria* cells and enhances bacterial actin-based motility. SH2-Bβ enhances actin-based movement of ActA-coated beads in a biomimetic actin-based motility assay, provided that VASP is present. In vitro binding assays show that SH2-Bβ binds ActA but not VASP; however, binding to ActA is greater in the presence of VASP. Because VASP also plays an essential regulatory role in actin-based processes in eukaryotic cells, the present results provide mechanistic insight into the functions of both SH2-Bβ and VASP in motility and also increase our understanding of the fundamental mechanism by which *Listeria* spreads.

Listeria monocytogenes is a facultative intracellular gram-positive bacterial pathogen that can invade a broad range of cell types and cause a variety of syndromes in humans and animals. Bacterial invasion of host cells starts by the interaction of *Listeria* with the plasma membrane, which progressively enwraps the bacterium. The bacterium escapes from the phagosome and freely proliferates within the host cell cytosol. Concomitant with bacterial replication, *Listeria* induces polymerization of host actin at its surface, leading to the formation of an actin tail. This tail propels the bacterium through the cytosol to neighboring cells (27, 45, 47). Actin and a limited subset of actin-binding proteins reconstitute bacterial motility in a purified system (25). However, beads covered with the listerial protein ActA move several times slower in this assay than in cells. This lower movement rate suggests that other proteins may also stimulate *Listeria* movement in cells. In this study, we introduce SH2-Bβ (Src homology 2 Bβ) as a protein that increases the efficiency of *Listeria* actin-based motility.

SH2-Bβ is a member of a widely expressed conserved family of adapter proteins containing several proline-rich regions, a central pleckstrin homology domain, and a C-terminal SH2 domain. SH2-Bβ binds, via its SH2 domain, to growth hormone-activated Janus tyrosine kinase (JAK2) (39) and to the activated receptor tyrosine kinases for insulin, insulin-like growth factor I, nerve growth factor, platelet-derived growth factor, and fibroblast growth factor (20, 33, 36, 37, 48). Several lines of evidence show that SH2-Bβ is involved in signaling to the actin cytoskeleton. First, SH2-Bβ increases membrane ruffling and pinocytosis induced by growth hormone, and a dominant-negative form of SH2-Bβ with a mutant SH2 domain decreases them. Second, SH2-Bβ is required for optimum actin-based cell motility and binds Rac (7, 18). Finally, Lnk and APS (an adaptive protein with a pleckstrin homology domain and an SH2 domain), other members of the SH2-B family of adapter proteins, have also been implicated as regulators of actin (17, 21). However, the mechanism by which the effects of SH2-B family proteins on the actin cytoskeleton are mediated remains largely unknown.

Cell protrusion is an elementary actin-based motility process that is reasonably understood at the molecular level. Filament treadmilling, regulated by actin-depolymerizing factor (ADF)/cofilin, profilin, and capping proteins, powers the forward movement of the leading edge. New filaments are constantly generated by signal-responsive Wiskott-Aldrich syndrome protein (WASP)/WAVE family proteins, which are targeted to the leading edge and use the Arp2/3 complex to branch filaments and stimulate actin assembly in a spatially controlled fashion. Actin-based propulsion of intracellular pathogens, such as *Listeria* and *Shigella*, is driven by the same mechanism. Filaments are branched at the bacterium surface either by N-WASP, recruited and activated by the *Shigella* protein IcsA (11), or by the *Listeria* protein ActA (8, 19), which works as a functional

* Corresponding author. Present address: Department of Biological Sciences, University of Toledo, 2801 W. Bancroft Street, Toledo, OH 43606-3390. Phone: (419) 530-7876. Fax: (419) 530-7737. E-mail: mdiakon@utnet.utoledo.edu.
† M.D. and E.H. contributed equally to this work.
‡ Present address: Departments of Microbiology & Internal Medicine, Ohio State University, Columbus, OH.
▽ Published ahead of print on 23 April 2007.

homolog of eukaryotic WASP family proteins (4, 42, 51). Particular interest has been given to *Listeria* because, in contrast to the case for *Shigella*, its efficient movement requires vasodilator-stimulated phosphoprotein (VASP) (24, 25, 43). Proteins of the Ena/VASP family are important regulators of cellular actin-based processes, such as cell migration, chemotaxis, axon guidance, and T-cell polarization. VASP localizes at focal contacts and at filopodial and lamellipodial tips (14, 22, 34, 35). Much of what we know about the effectors of VASP in motile processes has come from the *Listeria* system. The N-terminal EVH1 domain of VASP binds four FPPPP proline-rich repeats on ActA (4, 5, 26, 28, 32, 42, 43). In eukaryotic cells, VASP is thought to regulate filament branching by some unidentified cellular machinery using the Arp2/3 complex, since filaments at the leading edge are less densely branched in the presence of VASP than in its absence (3). Filaments that form actin tails initiated by ActA-coated beads placed in a reconstituted motility assay (40) are also less densely branched in the presence of VASP. Actin-based propulsion is reconstituted in vitro in a minimum biomimetic motility assay containing five pure proteins in which ActA- or N-WASP-coated beads move in a stationary fashion (25, 40, 52). VASP stimulates the motility of ActA-coated beads but does not affect the motility of N-WASP-coated beads.

To gain greater insight into the function of SH2-Bβ in motility, we examined the effect of SH2-Bβ on actin-based propulsion of *Listeria* in vivo and in vitro, using infected cells, cell extracts, and biomimetic motility assays. We show that SH2-Bβ is required for optimal movement of *Listeria* and that this function requires VASP. We also show that SH2-Bβ binds to ActA. Our data therefore reveal a new link between VASP and SH2-Bβ and open new perspectives on the functions of these two proteins in motile processes.

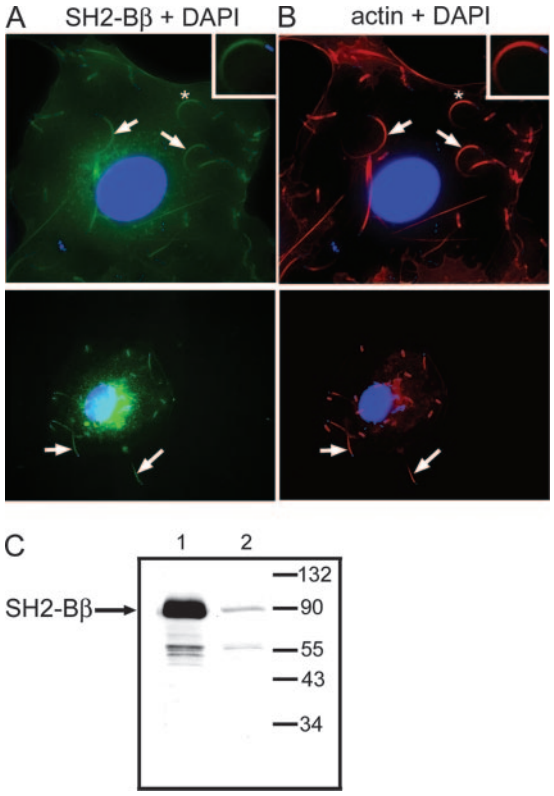

FIG. 1. Endogenous SH2-Bβ is present in *Listeria* actin tails. (A) COS-7 cells were infected with *Listeria* and stained with anti-SH2-Bβ (green), DAPI (blue), and phalloidin-Texas Red (red). Arrows indicate bacterial actin tails. Boxed regions in the upper right corners are enlarged images of the tails marked with asterisks in the larger images. (B) Macrophages were infected with *Listeria* and stained with anti-SH2-Bβ (green), DAPI (blue), and phalloidin-Texas Red (red). Arrows indicate bacterial actin tails. (C) Whole-cell lysates of COS-7 cells transfected with (lane 1) or without (lane 2) cDNA encoding SH2-Bβ were subjected to anti-SH2-Bβ Western blotting. The migration of endogenous SH2-Bβ and molecular weight standards is indicated.

MATERIALS AND METHODS

Plasmids, antibodies, and proteins. cDNAs encoding green fluorescent protein (GFP)-tagged SH2-Bβ, SH2-Bβ(R555E), SH2-Bβ(1-555), and SH2-Bβ(504-670), myc–SH2-Bβ, and glutathione *S*-transferase–SH2-Bβ (GST–SH2-Bβ) were described previously (36, 37). A cDNA encoding GFP-VASP was described previously (13). Polyclonal antibodies raised against SH2-Bβ (anti-SH2-Bβ) (39) were used for ratiometric analysis. Anti-VASP (Alexis), anti-myc (Santa Cruz Biotechnology, Inc.), Texas Red-phalloidin (Invitrogen), phalloidin-Alexa Fluor 488 (Invitrogen), and DAPI (4′,6′-diamidino-2-phenylindole; Invitrogen) were used for immunocytochemistry. Polyclonal anti-SH2-Bβ from Santa Cruz Biotechnology was used for immunocytochemistry and Western blotting. Anti-GFP was obtained from BD Biosciences. The actin used in motility, polymerization, and cosedimentation assays was purified from rabbit muscle (44) and isolated as calcium ATP–G-actin by gel filtration. Human ADF/cofilin and plasma gelsolin were expressed in *Escherichia coli* and purified (25). Profilin was purified from the bovine spleen (30). The Arp2/3 complex was purified from the bovine brain (11). His-tagged human VASP was expressed and purified from insect Sf9 cells, using the baculovirus expression system (24). His-tagged full-length ActA (ActA[1-584Rhis]) used for the motility assay was purified from cultures of *Listeria* strain BAC 093 (*Listeria monocytogenes* L028actA) (5). Human His-tagged N-WASP was expressed in Sf9 cells, using the baculovirus system (11).

Bacterial strains and culture conditions. Wild-type (WT) *Listeria* strain 1040S was used in most experiments. ΔActA6 *Listeria* strains DPL 2823 (in vitro experiments) and DPL 2374 (in vivo experiments), which express a mutant ActA protein lacking the proline-rich repeat region responsible for VASP binding, and strain DPL 2723, which constitutively produces His-ActA for ActA purification, were gifts of D. A. Portnoy (University of California at Berkeley, Berkeley, CA). Strain DPL 4087 (gift of J. A. Theriot, Stanford University, Stanford, CA), which constitutively produces ActA, was used for assays with *Xenopus* egg extract.

Immunocytochemistry and *Listeria* infection. COS-7 cells or bone marrow-derived murine macrophages grown on coverslips were infected with either a WT or ΔAct6 strain of *Listeria* (46). Coverslips were incubated with anti-SH2-Bβ followed by goat anti-rabbit–Oregon Green. The images presented are representative of at least three separate experiments. In all cases, staining by the secondary antibody reagent alone was negligible (not shown). For Fig. 6D, fluorescence intensities were calculated using MetaMorph software and averaged for 12 images of the long tails of *Listeria* organisms. For actin tail measurement, transiently transfected (by calcium phosphate precipitation) COS-7 cells were infected with *Listeria*, fixed, and stained with phalloidin-Texas Red or phalloidin-Alexa Fluor 488 and DAPI. GFP-positive cells were located using a fluorescein isothiocyanate (FITC) filter set. GFP-positive cells with approximately the same level of overexpression (judged by their brightness in a FITC channel) were chosen for imaging. Images were collected and analyzed by NIH Image software. Tails were measured in motile bacteria only. Several images from different focal planes were taken of tails that spanned more than one focal plane. Mouse embryo fibroblasts (MEF) from SH2-B$^{-/-}$ and SH2-B$^{+/+}$ mice were infected with *Listeria*, fixed, and stained with phalloidin-Texas Red and DAPI as described above. Data were pooled and analyzed using a two-tailed unpaired *t* test. For VASP localization, MEF were transfected with cDNA encoding GFP-VASP by using Fugene 6 (Roche) according to the manufacturer's protocol, infected with WT *Listeria*, and stained for actin as described above. Confocal imaging was performed with a Noran Oz laser scanning confocal microscope (Morphology and Image Analysis Core of MDRTC). The MV^{D7} cells derived from embryonic fibroblasts taken from MENA/VASP double knockout mice (2) were transfected as described above, infected with WT *Listeria*

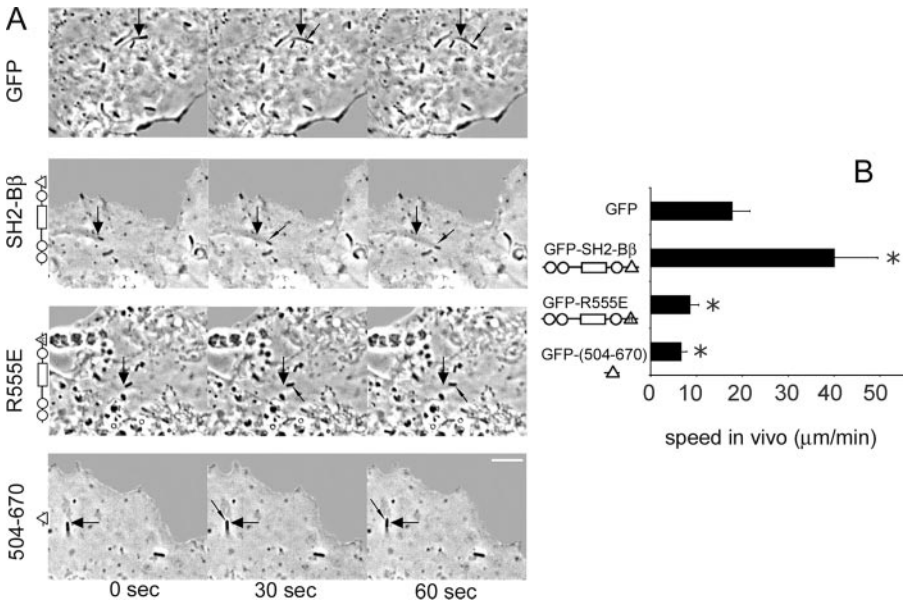

FIG. 2. SH2-Bβ enhances intracellular actin-dependent *Listeria* motility. (A) COS-7 cells were transfected with cDNA encoding either GFP alone or the indicated forms of GFP–SH2-Bβ. The large arrows refer to the initial position of the bacterium, while small arrows indicate the moving bacterium. In the schematic of SH2-Bβ, the circles represent proline-rich regions, the rectangle represents the pleckstrin homology domain, and the triangles represent the SH2 domain. Bar, 4 μm. (B) The movement of bacteria versus time was measured, and the velocity was calculated. Bars represent means plus standard errors of the means (SEM) [n = 13, 13, 10, and 14 for cells expressing GFP, GFP–SH2-Bβ, GFP–SH2-Bβ(R555E), and GFP–SH2-Bβ(504-670), respectively]. ∗, $P < 0.05$ compared to cells expressing GFP.

as described previously (13), and stained with phalloidin-Alexa Fluor 488 and anti-myc as described above.

Measurement of *Listeria* motility. COS-7 cells overexpressing GFP alone or a GFP-tagged form of SH2-Bβ were infected with *Listeria*. Transfected cells were located with a FITC filter set, and phase-contrast video images were collected (1 frame/15 seconds). Tracks of individual bacteria were measured over time, using MetaMorph software. Data were pooled and analyzed using a two-tailed unpaired *t* test.

A *Xenopus laevis* egg extract was prepared as previously described (46). Rhodamine–G-actin (Cytoskeleton Inc.) was subjected to a cycle of polymerization-depolymerization. *Listeria* constitutively secreting ActA was added to the *Xenopus* egg extract supplemented with rhodamine–G-actin and an ATP-regenerating mix. *Listeria* was visualized using a Nikon TE300 inverted microscope with shutter-controlled illumination. Images were recorded (1 frame/15 seconds), and *Listeria* speeds were quantified using MetaMorph software.

Some oocyte extracts were supplemented with GST or GST–SH2-Bβ purified using a glutathione-agarose affinity column (Sigma-Aldrich). The purity of the eluted GST or GST–SH2-Bβ was monitored by sodium dodecyl sulfate-polyacrylamide gel electrophoresis (SDS-PAGE), and the protein concentration was estimated by comparison to a Coomassie blue-stained bovine serum albumin (BSA) standard run in the same gel. The concentration of GST–SH2-Bβ was estimated to be 0.5 μM, which corresponds to the estimated concentration of endogenous SH2-Bβ in cells. Data were pooled and analyzed using a two-tailed unpaired *t* test.

ActA (or N-WASP)-coated beads and motility assay. Two-micrometer-diameter carboxylated polystyrene beads (Polysciences) in a suspension containing 0.25% solids were incubated with 1.5 μM ActA (or 400 nM N-WASP) in Xb buffer (10 mM HEPES, pH 7.8, 0.1 M KCl, 1 mM $MgCl_2$, 1 mM ATP, 0.1 mM $CaCl_2$, and 0.01% NaN_3) for 1 h on ice. BSA (1%) was added, and the incubation was continued for 15 min. Beads were washed in Xb buffer, stored on ice in Xb buffer with 0.1% BSA, and used within 4 to 5 days (40). The standard motility medium was composed of 7 μM actin, 5 μM ADF, 2.4 μM profilin, 90 nM gelsolin, and 100 nM Arp2/3 (25, 40), with or without VASP (25 to 150 nM) and with or without SH2-Bβ (0.5 to 1.4 μM). After 5 min, a steady state was reached, and functionalized beads were diluted 100-fold in motility medium. Up to four different motility assays could be run simultaneously on a single microscope slide by using a hydrophobic marker pen (Dakocytomation) to separate the samples. The chambers were closed with a coverslip (40 by 22 mm^2) and sealed with Valap (petrolatum-lanolin-paraffin [1:1:1]). All observations were performed on an Olympus AX70 microscope equipped with a charge-coupled device camera (Orca IIER; Hamamatsu) and a motorized stage (Märzhäuser). MetaMorph software (Universal Imaging Corp.) was used for image acquisition, stage control, and microscope control. Synchronous movies of up to four fields were

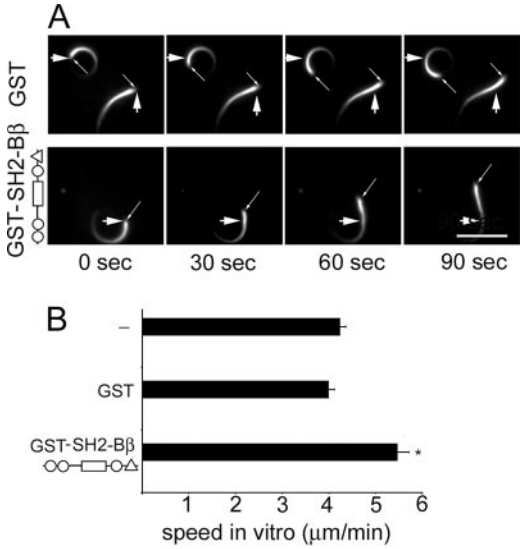

FIG. 3. SH2-Bβ enhances *Listeria* motility in *Xenopus* egg extract. (A) *Listeria* cells were incubated in *Xenopus* egg extracts supplemented with rhodamine-labeled G-actin and either GST or GST–SH2-Bβ. Large arrows indicate the initial position of the bacterium, and thin arrows indicate the moving bacterium. Bar, 8 μm. (B) The movement of bacteria versus time was measured, and the velocity was calculated. Bars represent means plus SEM (n = 8, 12, and 17 for extracts without supplementation and those supplemented with GST and GST–SH2-Bβ, respectively). ∗, $P < 0.05$ compared to extracts supplemented with GST.

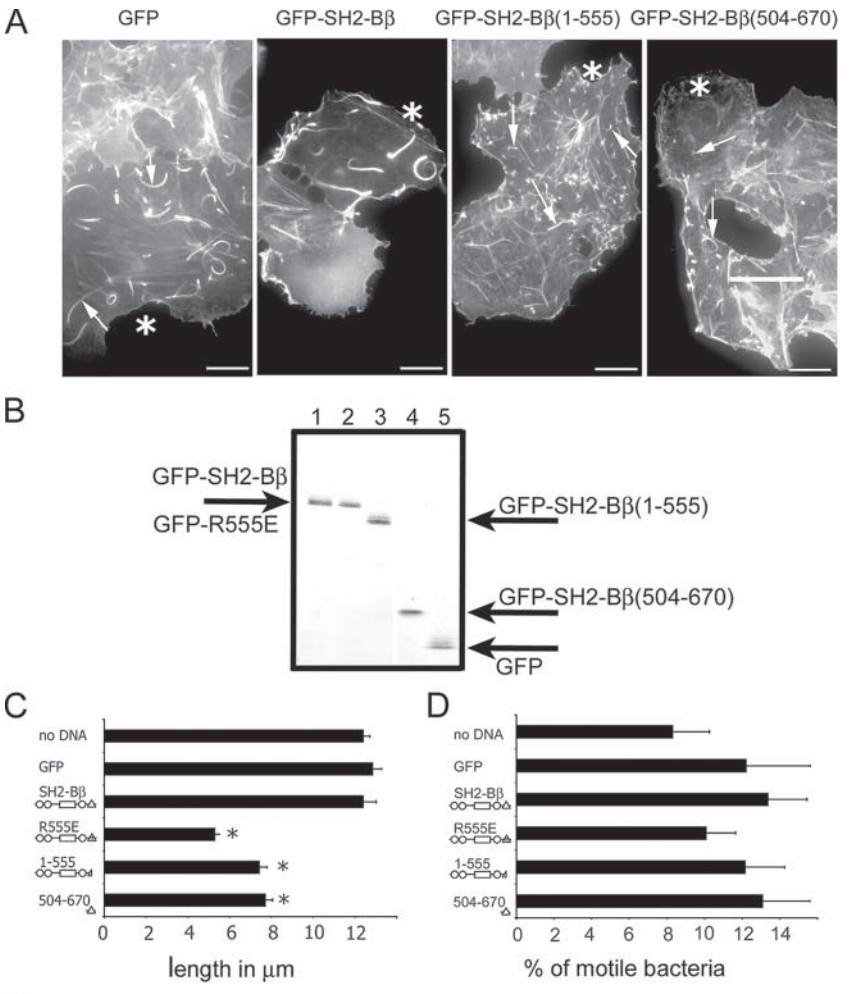
A
GFP
GFP-SH2-Bβ
GFP-SH2-Bβ(1-555)
GFP-SH2-Bβ(504-670)
B
1 2 3 4 5
GFP-SH2-Bβ
GFP-R555E
GFP-SH2-Bβ(1-555)
GFP-SH2-Bβ(504-670)
GFP
C
no DNA
GFP
SH2-Bβ
R555E
1-555
504-670
0 2 4 6 8 10 12
length in μm
D
no DNA
GFP
SH2-Bβ
R555E
1-555
504-670
0 2 4 6 8 10 12 14
% of motile bacteria
E
WT
R555E
(1-555)
(504-670)
F
SH2-B +/+
SH2-B -/-
0 1 2 3 4 5 6 7
length in μm
SH2-B +/+
SH2-B -/-
0 1 2 3 4
speed in μm/min

recorded (1 frame/30 s) using MetaMorph software. After the addition of the ActA beads (starting time [t_0]), the time needed to choose the fields and enter their positions was approximately 5 to 15 min. The acquisition times (t) of the images/movies indicated in this paper include this delay time. For each sample, a minimal set of five beads was selected, the beads were tracked using Metamorph software, and their individual mean velocities were calculated over the total acquisition time. The average velocity was calculated over the set of beads. Day-to-day discrepancies in velocity measurement can occur due to differences in activity of the motility medium components. To avoid this problem, comparative velocity measurements were done with one single varying parameter, and all assays of one series were performed on the same day. The curves plotted in the figures represent single series of motility assays, i.e., each point corresponds to a single sample of five beads or more. The number (n) of tracked beads for each point is given in the figure legends.

Cosedimentation assay with F-actin. Actin (3 μM; 10% pyrenyl labeled) was polymerized by the addition of 0.1 M KCl, 1 mM $MgCl_2$, and 0.2 mM EGTA to G-actin. Polymerization was carried out in the absence or in the presence of 0.5 μM GST–SH2-Bβ supplemented with 50 nM Arp2/3 complex and 40 nM ActA, with or without 50 nM VASP. Polymerization was monitored by the increase in pyrene fluorescence. Once polymerization was completed, filaments were sedimented at 400,000 × g for 20 min at 20°C. The presence of GST–SH2-Bβ in pellets and supernatants was detected either by immunodetection using polyclonal anti-GST (Sigma) or by Coomassie blue staining of an SDS-PAGE gel (that allowed simultaneous detection of actin). Quantification of the data was carried out by scanning the gels and immunoblots and integrating the band intensities using ImageJ software.

Immunoblotting and pull-down assay. GFP, GFP-tagged SH2-Bβ, and the indicated SH2-Bβ mutants were expressed in COS-7 cells and immunoprecipitated from cell lysates, using anti-GFP, rabbit anti-mouse immunoglobulin G, and protein A-agarose. GFP-tagged proteins were visualized by immunoblotting with anti-GFP.

For pull-down assays, 1 μM of a potential binding partner of SH2-Bβ (ActA, VASP, or the Arp2/3 complex, as indicated) was mixed with either 1 μM GST–SH2-Bβ or 1 μM GST in a reaction volume completed to 100 μl with buffer B (20 mM Tris, pH 7.8, 100 mM KCl, 1 mM $MgCl_2$, 100 μM $CaCl_2$, and 0.1% Tween) and then incubated for 1 h at 4°C. The reaction mixtures were added to 20 μl of glutathione-Sepharose beads and incubated for 1 h at 4°C, with stirring. Supernatants were collected, and glutathione-Sepharose beads were washed three times with buffer B. Free and bound proteins were detected by immunodetection, using a monoclonal anti-VASP antibody and polyclonal anti-ActA and anti-Arp3 antibodies. Quantification of the data was carried out as described above.

Actin polymerization assay. Actin (3 μM; 10% pyrenyl labeled) was polymerized in the presence of 25 nM Arp2/3 complex and ActA-coated beads (1-μm diameter; 0.031% solid suspension) (40), with or without 106 nM VASP and with or without 0.47 μM GST–SH2-Bβ, in F-actin buffer (5 mM Tris-HCl, pH 7.8, 1 mM dithiothreitol, 0.2 mM ATP, 0.1 mM $CaCl_2$, 0.1 M KCl, and 1 mM $MgCl_2$). Polymerization was monitored by the increase in pyrene fluorescence, using a Safas spectrofluorimeter allowing simultaneous recording of up to 10 samples.

RESULTS

Endogenous SH2-Bβ is present in *Listeria* actin tails. We previously observed that the adapter protein SH2-Bβ colocalizes with actin in motile regions of mammalian cells (18) and enhances cell motility (7). These observations suggested that SH2-Bβ may enhance cell motility by interacting directly with actin and/or actin-regulating proteins and led us to predict that SH2-Bβ would be present in *Listeria* actin tails and enhance the motility of *Listeria*. To test this, primary murine macrophages (Fig. 1B) or COS-7 (Fig. 1A) cells were infected with *Listeria* and stained with anti-SH2-Bβ. Endogenous SH2-Bβ localized in *Listeria* actin tails in both cell lines. Additionally, both GFP-tagged (see Fig. 4E) and myc-tagged (see Fig. 6E) SH2-Bβ also localized in *Listeria* tails. Immunoblotting of whole-cell lysates of COS-7 cells overexpressing myc–SH2-Bβ (Fig. 1C, lane1) or COS-7 cells expressing endogenous SH2-Bβ only (Fig. 1C, lane 2) revealed that anti-SH2-Bβ shows high specificity for SH2-Bβ. Ratiometric analysis (18) using anti-SH2-Bβ–FITC to identify SH2-Bβ and sulfonyl chloride-Texas Red to stain the cytoplasm allowed us to visualize in white the regions of the cell where anti-SH2-Bβ–FITC was concentrated and confirmed the specificity of SH2-Bβ localization in the actin tails (data not shown).

SH2-Bβ enhances actin-based *Listeria* motility in cells and in cell extracts. *Listeria* movement was recorded in infected COS-7 cells overexpressing SH2-Bβ. COS-7 cells were transfected with cDNA encoding GFP alone or GFP fused to either SH2-Bβ, the SH2 domain-defective mutant SH2-Bβ(R555E), or the C terminus of SH2-Bβ (504-670), containing primarily the SH2 domain (Fig. 2A). In SH2-Bβ(R555E), the critical Arg (R) within the FLVR motif of the SH2 domain is mutated to Glu (E). Both mutants have been shown to decrease ligand-induced cell ruffling and motility (7, 18). In control cells expressing GFP, the bacteria moved at an average speed of 17.9 μm/min, similar to rates reported previously (23, 43, 46) (Fig. 2). Strikingly, in cells overexpressing SH2-Bβ, the bacteria moved more than twice as fast (40.1 μm/min). In contrast, in cells expressing the SH2 domain-defective mutant SH2-Bβ(R555E) or the C terminus of SH2-Bβ (504-670), *Listeria* movement was slowed down (8.7 μm/min and 6.7 μm/min, respectively). These data demonstrate that SH2-Bβ substantially enhances *Listeria* motility and that both the SH2 domain

FIG. 4. SH2-Bβ affects the length of *Listeria* actin tails. (A) COS-7 cells expressing the indicated proteins were infected with *Listeria* and stained for actin. Asterisks denote transfected cells. Arrows indicate *Listeria* actin tails. Bars, 10 μm. (B) GFP–SH2-Bβ (lane 1), GFP–SH2-Bβ(R555E) (lane 2), GFP–SH2-Bβ(1-555) (lane 3), GFP–SH2-Bβ(504-670) (lane 4), and GFP (lane 5) were overexpressed in COS-7 cells. GFP and GFP-tagged forms of SH2-Bβ were immunoprecipitated using anti-GFP and visualized by blotting with anti-GFP. The migration of GFP and GFP-tagged forms of SH2-Bβ is indicated. (C) Lengths of actin tails of *Listeria* in cells expressing the indicated forms of SH2-Bβ. n = 280, 117, 98, 95, 102, and 119 for nontransfected cells and cells expressing GFP, GFP–SH2-Bβ, GFP–SH2-Bβ(R555E), GFP–SH2-Bβ(1-555), and GFP–SH2-Bβ(504-670), respectively. (D) The number of *Listeria* organisms with actin tails as a percentage of *Listeria* organisms per cell was determined for cells expressing the indicated forms of GFP–SH2-Bβ. n = 24, 15, 21, 16, 18, and 25 for nontransfected cells and cells overexpressing GFP, GFP–SH2-Bβ, GFP–SH2-Bβ(R555E), GFP–SH2-Bβ(1-555), and GFP–SH2-Bβ(504-670), respectively. (E) COS-7 cells expressing the indicated GFP-tagged proteins (white) were infected with *Listeria* and stained with DAPI (blue) and phalloidin-Texas Red (not shown). Arrows indicate GFP–SH2-Bβ in long bacterial tails and GFP-tagged SH2-Bβ(R555E), SH2-Bβ(1-555), and SH2-Bβ(504-670) in short *Listeria* tails. *, plasma membrane. Bar, 5 μm. (F) The lengths of actin tails of *Listeria* were determined in MEF from SH2-$B^{+/+}$ and SH2-$B^{-/-}$ mice. n = 245 for +/+ MEF and 344 for −/− MEF. The movement of bacteria in MEF from SH2-$B^{+/+}$ (n = 123) and SH2-$B^{-/-}$ (n = 179) mice versus time was measured, and velocities were calculated. For panels C, D, and F, bars represent means plus SEM for three independent experiments. *, $P < 0.05$ compared to cells expressing GFP (B) or to MEF from SH2-$B^{+/+}$ mice (F).

and the N terminus of SH2-Bβ are required for this stimulatory effect.

Xenopus laevis egg extracts supplemented with rhodamine-actin were used to assess whether direct addition of SH2-Bβ would increase *Listeria* motility in a cell-free system (Fig. 3). The average rate of *Listeria* movement in these extracts was 4 μm/min, similar to rates reported previously (43, 46). Upon addition of 0.5 μM GST–SH2-Bβ, the *Listeria* speed increased to 5.47 μm/min, whereas it was unaffected by the addition of 0.5 μM GST. These results suggest that SH2-Bβ acts directly on *Listeria* actin tails to increase *Listeria* motility.

Dominant-negative forms of SH2-Bβ cause shortening of *Listeria* actin tails. The length of *Listeria* actin tails, which correlates with bacterial speed (45), was measured in cells overexpressing SH2-Bβ. COS-7 cells were transfected with cDNA encoding GFP alone or GFP fused to SH2-Bβ, SH2-Bβ(504-670), SH2-Bβ(R555E), or an additional SH2 domain-deficient mutant, SH2-Bβ(1-555), that lacks most of the SH2 domain and has been shown to have a similar inhibitory effect to that of SH2-Bβ(R555E) on ligand-induced cell ruffling and motility (7, 18) (Fig. 4A). Western blot analysis confirmed similar levels of expression of GFP and GFP-tagged SH2-Bβ, SH2-Bβ(504-670), SH2-Bβ(R555E), and SH2-Bβ(1-555) (Fig. 1B), while immunofluorescence analysis revealed that all of the SH2-Bβ mutants, like WT SH2-Bβ, localize in *Listeria* tails (Fig. 4E). Tail lengths were determined using images from several different focal planes. Identical tail lengths were recorded for cells overexpressing SH2-Bβ, nontransfected cells, and cells expressing GFP alone (Fig. 4A and C). In contrast, in cells expressing forms of SH2-Bβ lacking a functional SH2 domain as well as cells expressing only the SH2 domain and the C terminus of SH2-Bβ, *Listeria* exhibited much shorter actin tails. The percentages of bacteria that were motile, however, were similar for all cells (Fig. 4D). These data showing an inhibitory effect of SH2-Bβ(504-670) and SH2-Bβ(R555E) on tail length are consistent with the inhibitory effect of these mutants on *Listeria* motility shown in Fig. 2, as predicted from a previous report linking *Listeria* tail length to *Listeria* motility in PtK2 cells (45). However, overexpression of SH2-Bβ promoted a large increase in speed without significantly increasing actin tail length. This suggests that while tail length correlates with speed when the rate of actin depolymerization is unchanged, upon overexpression of SH2-Bβ, the rates of both actin polymerization and depolymerization are increased.

The absence of SH2-B results in decreased *Listeria* motility. To confirm a contribution of endogenous SH2-B to *Listeria* motility, *Listeria* motility and tail length were assessed in infected MEF from control mice and from SH2-B knockout mice lacking all known isoforms of SH2-B (9, 10). In confirmation of SH2-Bβ stimulating *Listeria* motility, *Listeria* movement was slower in SH2-$B^{-/-}$ cells than in SH2-$B^{+/+}$ cells (Fig. 4F). In addition, the length of *Listeria* actin tails in SH2-$B^{-/-}$ cells was statistically significantly shorter than that in SH2-$B^{+/+}$ cells (Fig. 4F).

VASP is required for the stimulatory effect of SH2-Bβ on actin-based motility of *Listeria* in cell extracts and in a reconstituted motility assay. VASP is known to be required for efficient movement of *Listeria* both in vivo and in vitro. To address the possible interplay between VASP and SH2-Bβ on *Listeria* motility, we used a *Listeria* ΔActA6 strain that expresses a mutant ActA protein lacking the proline-rich repeat region that interacts with the EVH1 domain of VASP (43). In agreement with the work of Smith et al. (43), we found that the motility of the ΔActA6 strain in *Xenopus* egg extracts (which contain endogenous VASP) was decreased compared to that of WT *Listeria* (Fig. 5A). The addition of GST–SH2-Bβ increased the motility of WT *Listeria* but not that of ΔActA6 *Listeria*. This result suggests but does not prove that VASP binding to ActA is required for the stimulatory effect of SH2-Bβ.

To determine whether VASP binding to nonmutated ActA is normally required for the stimulatory effect of SH2-Bβ on WT *Listeria* motility, a chemically controlled biomimetic motility assay was used. The actin-based movement of ActA-coated beads was monitored in a minimal reconstituted medium containing actin, the Arp2/3 complex, gelsolin, ADF, and profilin, with or without VASP (25) (Fig. 5B and C). As previously reported (40), in the absence of VASP, beads moved at a very low rate (~1 to 1.5 μm/min), often irregularly. The addition of 1 μM GST–SH2-Bβ, GST, or GST–SH2-Bβ(504-670) did not change the speed of the beads or the morphology of the tails. The addition of 150 nM VASP alone increased the speed of ActA-beads to ~2.5 μm/min. Bead velocity was maintained at this high level for over 1 h. VASP also changed the morphology of the actin tail, making it looser. Notably, the addition of SH2-Bβ with VASP further increased the speed of ActA-coated beads, up to ~5 μm/min. SH2-Bβ also caused the actin tails to become denser and tighter, though not as tight and dense as the actin tails in the absence of both VASP and SH2-Bβ (Fig. 5C). The dependence of bead velocity on the concentration of VASP was examined in the presence and absence of 1 μM SH2-Bβ (Fig. 5D). SH2-Bβ stimulated the VASP-induced increase of the bead velocity, and this effect was more pronounced at the lowest concentration, 25 nM, which is physiologically relevant (~9 μm/min). The addition of increasing concentrations of SH2-Bβ (0 to 1.5 μM) to motility medium supplemented with 50 nM VASP induced an increase of the velocity to ~7 μm/min (data not shown). The intriguing effect of SH2-Bβ on the VASP-dependent motility of ActA-coated beads suggested that SH2-Bβ requires VASP for its function on *Listeria* motility. To provide additional support for this conclusion, a second biomimetic motility assay was done using beads coated with N-WASP, a protein from the WASP family that is used by *Shigella* and does not require VASP for motility. The movement of N-WASP-coated beads was not affected by SH2-Bβ, with or without 150 nM VASP (Fig. 5E).

We next tested the interdependence of VASP and SH2-Bβ binding to *Listeria*. We first visualized endogenous VASP and SH2-Bβ by immunofluorescence of *Listeria* tails in COS-7 cells. In agreement with previous reports, VASP was concentrated at the pole of the bacterium associated with the formation of new actin filaments (Fig. 6A to C). Endogenous SH2-Bβ colocalized with endogenous VASP at the interface between the bacterium and the actin tail in newly formed short actin tails (or actin "caps") (Fig. 6A and B, yellow areas and arrows). In motile bacteria with longer actin tails, SH2-Bβ still colocalized with VASP (Fig. 6B and C, yellow areas and arrows) at the interface between the bacterium and the actin tail. However, SH2-Bβ was also present along the tails, raising the possibility that SH2-Bβ translocates from the bacterial surface to the actin tail as the tail elongates. Quantification of fluores-

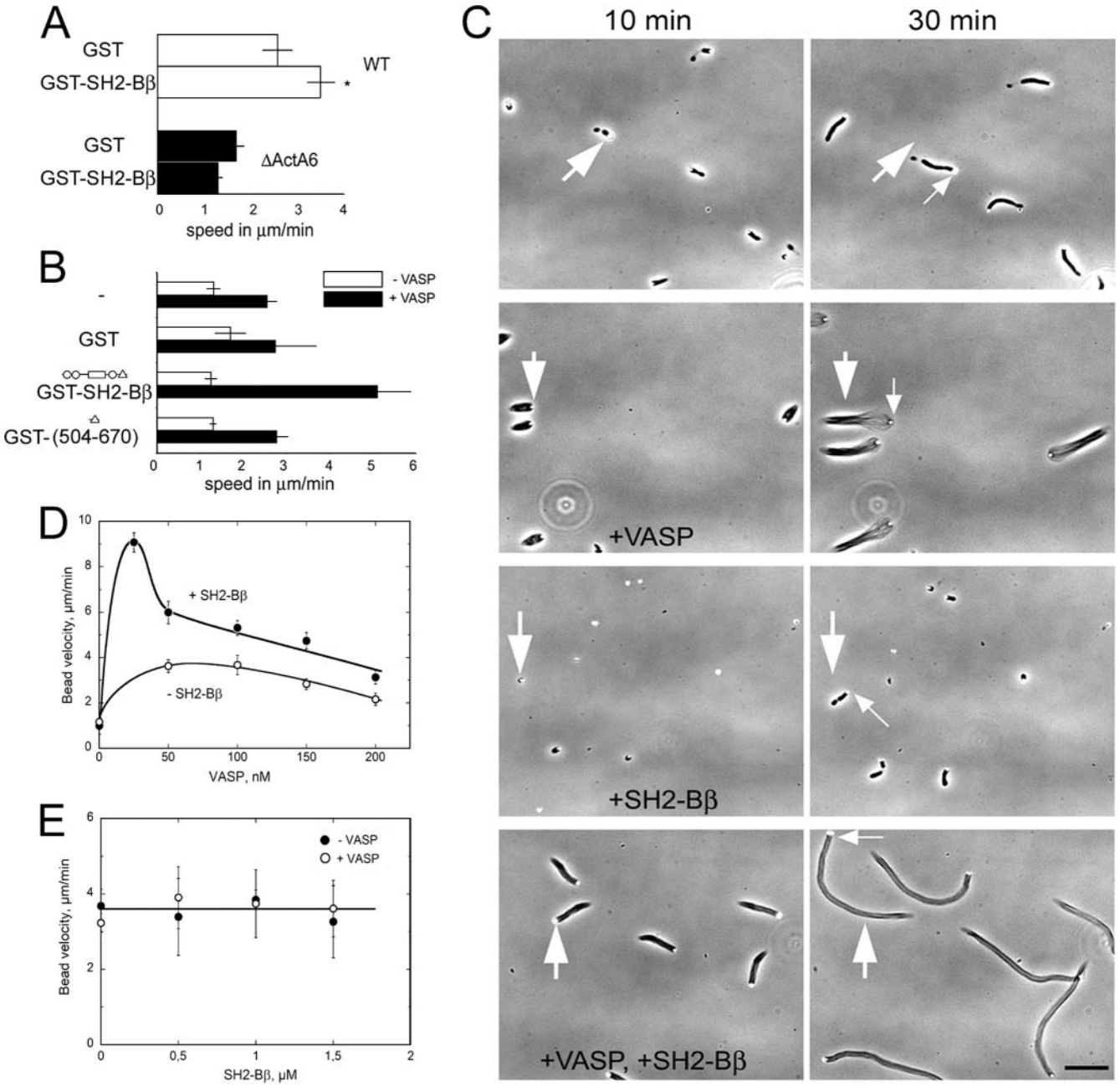

FIG. 5. VASP is required for the effect of SH2-Bβ on actin-based motility. (A) WT or ΔActA6 *Listeria* cells were incubated in *Xenopus* egg extract supplemented with either GST or GST–SH2-Bβ. The movement of individual bacteria was measured, and velocities were calculated. Bars represent means plus SEM. *, $P < 0.05$ compared to extracts supplemented with GST. (B) ActA-coated beads were incubated in motility medium, with or without 150 nM VASP and 1 μM of the indicated proteins. For each assay, the movement of n beads was measured, and the average velocity was calculated. From top to bottom, $n = 5$, 6, 6, and 4 without VASP and $n = 7$, 7, 8, and 8 with VASP. Bars represent means plus standard deviations (SD). (C) Time-lapse images of ActA-coated bead movement in motility medium, with or without 150 nM VASP and/or 1 μM SH2-Bβ, as indicated. The large arrows refer to the initial position of the bead, while small arrows indicate the moving bead. Flows in the samples sometimes induced a drift of the objects. Bar, 40 μm. (D) The velocity of ActA-coated beads was determined in motility medium supplemented with increasing concentrations of VASP in the presence (solid circles) or absence (open circles) of 1 μM SH2-Bβ. Bars represent means ± SD, calculated for a set of n beads in each sample. For increasing concentrations of VASP, $n = 7$, 5, 8, 6, 8, and 11 with SH2-Bβ and $n = 5$, 5, 9, 8, and 10 without SH2-Bβ. (E) The velocity of N-WASP-coated beads was determined in motility medium supplemented with increasing concentrations of SH2-Bβ in the presence (open circles) or absence (solid circles) of 150 nM VASP. The bead movement was independent of VASP and SH2-Bβ. Bars represent means ± SD, calculated for a set of n beads. For increasing concentrations of SH2-Bβ, $n = 10$, 13, 14, and 13 without VASP and $n = 9$, 6, 5, and 7 with VASP.

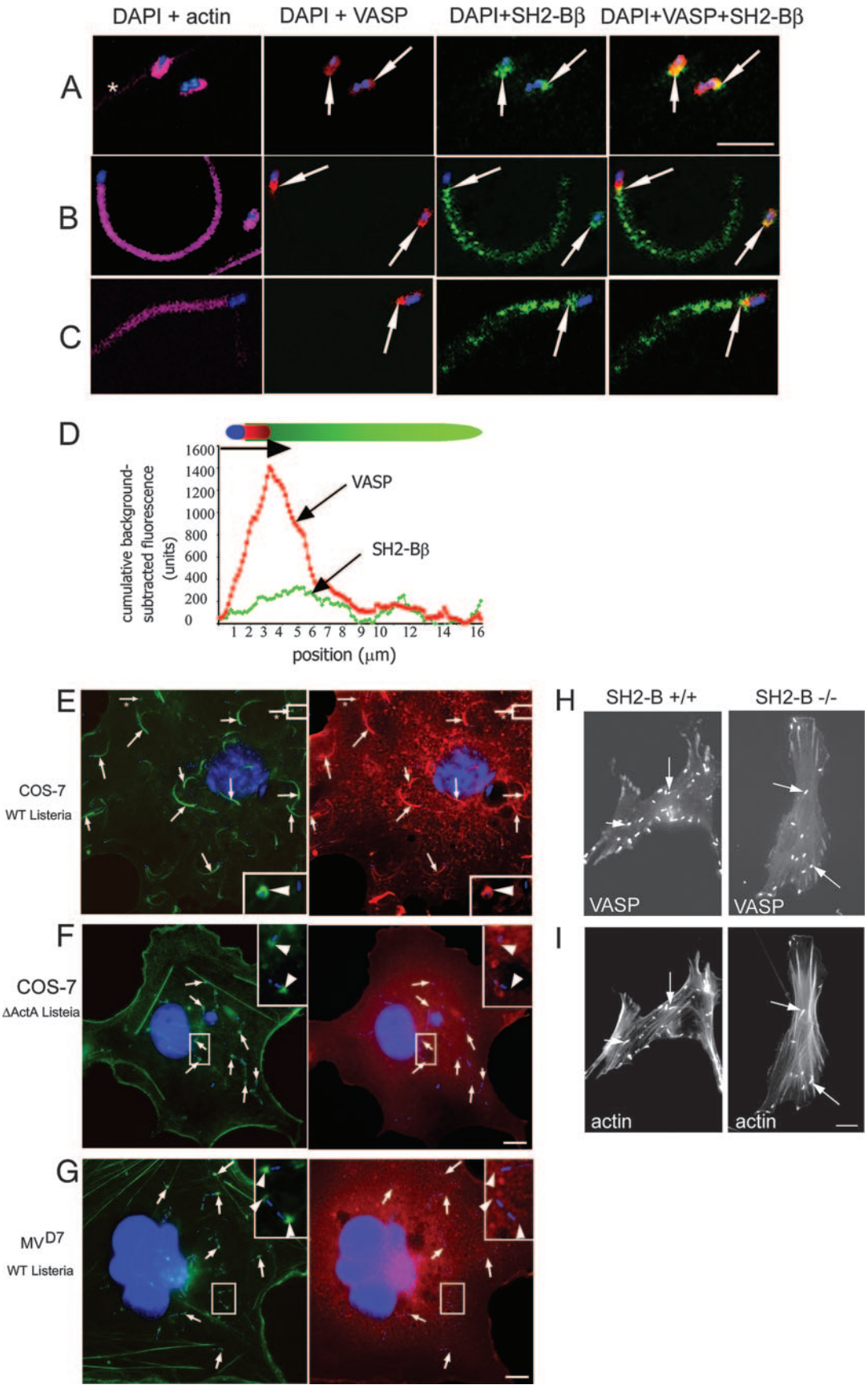
DAPI + actin
DAPI + VASP
DAPI+SH2-Bβ
DAPI+VASP+SH2-Bβ
A
B
C
D
cumulative background-subtracted fluorescence (units)
1600
1400
1200
1000
800
600
400
200
0
VASP
SH2-Bβ
1 2 3 4 5 6 7 8 9 10 12 14 16
position (μm)
E
COS-7
WT Listeria
F
COS-7
ΔActA Listeia
G
MV^D7
WT Listeria
H
SH2-B +/+
SH2-B -/-
VASP
VASP
I
actin
actin

cence intensity confirmed the partial colocalization of VASP and SH2-Bβ at the bacterium-tail interface (Fig. 6D). Why SH2-Bβ appears to distribute in a punctate manner in Fig. 6B and C is not known, but the effect may be antibody specific, since myc–SH2-Bβ was found to be distributed evenly along the actin tail. To determine whether VASP is required for the function of SH2-Bβ in *Listeria* motility, we looked to see if SH2-Bβ was present in actin tails of ΔActA6 *Listeria*, which lacks a VASP binding site in ActA, in COS-7 cells and of WT *Listeria* in MV^{D7} cells derived from embryonic fibroblasts from MENA/VASP double knockout mice (2). Neither myc–SH2-Bβ (Fig. 6F) nor GFP–SH2-Bβ (not shown) was present in the short actin tails of ΔActA6 *Listeria*, although they were visible in both short and long actin tails of WT *Listeria* (Fig. 1 and 6A to C and E). As reported previously, *Listeria* induced the formation of very short actin tails, or "caps," in MV^{D7} cells (13). Neither myc–SH2-Bβ (Fig. 6G) nor GFP–SH2-Bβ (not shown) was also present in these actin caps. In contrast, GFP-VASP was detected to similar extents in WT *Listeria* tails in infected MEF from both SH2-$B^{-/-}$ and SH2-$B^{+/+}$ mice (Fig. 6H and I). Thus, in vivo results support the conclusion derived from biomimetic motility assays, i.e., that the stimulatory effect of SH2-Bβ on bacterial motility depends on the recruitment of VASP to the surfaces of *Listeria* cells but that recruitment of VASP to the surfaces of *Listeria* cells does not require SH2-Bβ.

SH2-Bβ binding partners in actin-based motility. The fact that SH2-Bβ is detected in actin tails only if VASP is present is intriguing and raises a challenging issue regarding the molecular mechanisms by which VASP itself, as well as SH2-Bβ, affects motility and by which VASP and SH2-Bβ have a synergistic effect. Indeed, in most in vivo studies performed so far to address the function of VASP, endogenous SH2-Bβ was present. In living cells, VASP is found at focal adhesions (16). VASP also localizes at lamellipodial tips of motile cells, in amounts that correlate with the velocity of the leading edge (35). Filaments in lamellipodia (3) as well as in tails of ActA-coated beads moving in the biomimetic motility assay (40) appear to be less densely branched in the presence of VASP than in its absence. These observations suggest that VASP has similar functions in cell- and *Listeria* actin-based motility. The molecular mechanism accounting for these effects of VASP is not clear. The fact that SH2-Bβ synergizes with VASP may offer a clue to understanding the functions of these two proteins in vivo. In this endeavor, we sought possible partners of SH2-Bβ in the formation of an actin tail. The fact that the effects of SH2-Bβ are recapitulated in a minimum medium containing only five proteins restrains the number of putative targets of SH2-Bβ.

Polymerization assays showed that SH2-Bβ did not affect spontaneous actin assembly monitored by either pyrenyl-actin fluorescence or light scattering (data not shown). When actin was polymerized in branched filaments, using soluble ActA and the Arp2/3 complex, SH2-Bβ had no effect in the absence or presence of VASP. When polymerization in branched filaments was induced using ActA-bound beads, VASP displayed a large activation of branched polymerization (Fig. 7A), as previously reported (40), but this effect was not increased by SH2-Bβ.

Binding of SH2-Bβ to pure F-actin was tested in a sedimentation assay (Fig. 7B). We detected a fraction (~30%) of SH2-Bβ bound to F-actin (Fig. 7B, lane 3), in agreement with the observed association of SH2-Bβ with *Listeria* actin tails in cells and cell extracts. The equilibrium dissociation constant of SH2-Bβ for binding to F-actin was roughly estimated from this binding assay to be around 5 to 10 μM. SH2-Bβ did not cause depolymerization of F-actin in this assay, indicating that it does not bind G-actin. Accordingly, GST–SH2-Bβ did not bind to biotin–G-actin immobilized on streptavidin-derivatized beads (data not shown). When polymerization of actin in branched filaments was stimulated in the presence of soluble ActA and Arp2/3, the amount of SH2-Bβ bound to F-actin was not altered, even by the addition of VASP (Fig. 7B, lanes 4 and 5). At least 95% of the actin sedimented in all samples, independent of the addition of VASP, ActA, or SH2-Bβ.

Direct binding of SH2-Bβ to VASP and ActA was assayed using a pull-down assay with GST–SH2-Bβ bound to glutathione-Sepharose beads (Fig. 7C and D). The following observations were made. First, SH2-Bβ does not bind directly to VASP (Fig. 7C, bottom panel, lane 2). Pull-down experiments with in vitro-translated, [^{35}S]methionine-labeled SH2-Bβ and His-VASP immobilized on Ni-agarose also failed to detect direct binding of SH2-Bβ to VASP (data not shown). Second, SH2-Bβ binds ActA. Stronger binding of SH2-Bβ to ActA was recorded in the presence of VASP (Fig. 7C and D). While VASP did not interact directly with SH2-Bβ, it bound indirectly to the GST–SH2-Bβ

FIG. 6. SH2-Bβ colocalizes with VASP and requires VASP for localization with actin. (A to C) COS-7 cells were infected with *Listeria*, stained with anti-SH2-Bβ (green), anti-VASP (red), phalloidin-Texas Red (pink), and DAPI (blue), and imaged by confocal microscopy. VASP colocalizes with SH2-Bβ on the side of the bacterium (A and B, yellow areas and arrows) and the beginning of the tail (B and C, yellow areas and arrows). *, the plasma membrane. Bar, 5 μm. (D) Cumulative fluorescence intensities for VASP (red) and SH2-Bβ (green) in the long actin tails were background subtracted and plotted as a function of position. (E and F) COS-7 cells overexpressing myc–SH2-Bβ were infected with either a WT (E) or ΔActA6 strain (F) of *Listeria*. Actin tails and actin caps at one bacterial pole were visualized by phalloidin-Alexa Fluor 488 (green, arrows), and myc–SH2-Bβ was visualized with an anti-myc antibody (red). Arrows from the images stained for actin and bacteria were superimposed on the images stained for myc–SH2-Bβ and bacteria and demonstrate that myc–SH2-Bβ localizes in the long actin tails and the actin caps formed by WT but not ΔActA *Listeria*. The boxed regions in the right corners are enlarged images of the marked areas in the larger images. Arrowheads from the images stained for actin and bacteria were superimposed on the images stained for SH2-Bβ and bacteria. Arrows with asterisks indicate actin caps formed by WT *Listeria*. Bar, 10 μm. (G) MV^{D7} fibroblasts were infected with WT *Listeria*. Actin caps were visualized by phalloidin-Alexa Fluor 488 (green, arrows), and myc–SH2-Bβ was visualized with anti-myc antibody (red). Arrows were superimposed as described above to demonstrate that there is no colocalization of these two proteins. The boxed regions in the upper right corners are enlarged images of the marked areas in the larger images. Arrowheads from the images stained for actin and bacteria were superimposed on the images stained for myc–SH2-Bβ and bacteria. Bar, 10 μm. (H and I) MEF from SH2-$B^{+/+}$ (D) and SH2-$B^{-/-}$ (E) mice overexpressing GFP-VASP were infected with WT *Listeria* and stained for F-actin. GFP-VASP was localized at the poles of bacteria in both cell types. Arrows indicate actin tails (lower images) and GFP-VASP (upper images). Bar, 10 μm.

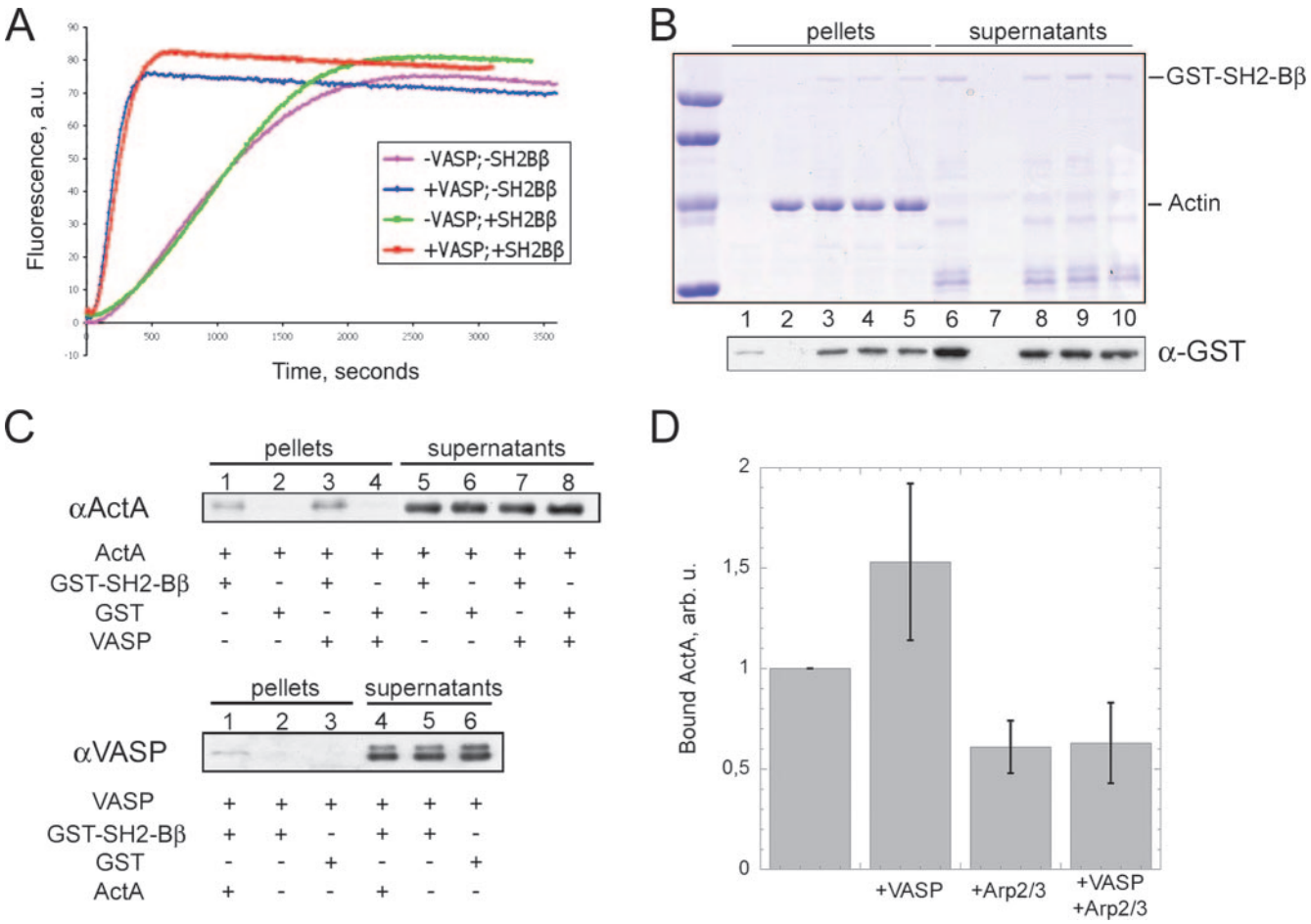

FIG. 7. Interaction of SH2-Bβ with actin and ActA. (A) Actin (3 μM; 10% pyrenyl labeled) was polymerized in the presence of ActA-coated beads and the Arp2/3 complex (20 nM), with or without VASP (107 nM) and with or without SH2-Bβ (0.5 μM). Polymerization was monitored by the increase in fluorescence intensity of pyrenyl-actin. a.u., arbitrary units. (B) Actin was polymerized in the presence of SH2-Bβ and additional proteins. F-actin and G-actin were separated by high-speed centrifugation, and the proteins present in pellets (lanes 1 to 5) and supernatants (lanes 6 to 10) were detected by SDS-PAGE (top). Additional bands in the supernatants (lanes 6 and 8 to 10) are degraded forms of SH2-Bβ that do not bind F-actin, confirming that specific binding is observed in lanes 3 to 5. Immunoblotting using anti-GST antibody was done to detect SH2-Bβ with a higher contrast (bottom). Actin was polymerized alone (lanes 2 and 7), in the presence of 0.5 μM SH2-Bβ (lanes 3 and 8), or supplemented with 50 nM Arp2/3 complex and 40 nM ActA, without (lanes 4 and 9) or with (lanes 5 and 10) 50 nM VASP. The control without actin (lanes 1 and 6) shows a slight contamination (<5%) of the pellet by SH2-Bβ that is negligible compared to the amount of SH2-Bβ (~30%) recruited by F-actin. (C) Pull-down assays of ActA and VASP with SH2-Bβ. (Top) ActA binds to GST–SH2-Bβ in the absence (lane 1) and, more strongly, in the presence (lane 3) of VASP. No ActA was detected in the negative controls (GST alone) (lanes 2 and 4). (Bottom) VASP alone (lane 2) does not bind to GST–SH2-Bβ beads and is recruited only via its strong interaction with ActA (lane 1). (D) Binding of ActA to SH2-Bβ as a function of Arp2/3 and VASP. In each experiment, the amount of ActA bound to GST–SH2-Bβ in the absence of other ligands is taken as a reference and normalized to 1 (left bar). The addition of VASP increased the amount of bound ActA by 50%. The addition of Arp2/3 induced a decrease of ~40%, with or without VASP. Bars represent means plus SD, computed from three independent experiments.

beads in the presence of ActA, presumably due to the strong interaction of its EVH1 domain with the proline-rich region of ActA.

ActA is a functional homolog of proteins of the WASP family that catalyze filament branching, using the Arp2/3 complex as a substrate (31, 40, 49–51). The first step in filament branching is binding of Arp2/3 to WASP or ActA in a ternary complex called the "branching complex," which then interacts with an actin filament to catalyze branching. When GST–SH2-Bβ beads were incubated with ActA in the presence of the Arp2/3 complex, less ActA was found bound to SH2-Bβ than in its absence, either in the presence or absence of VASP (Fig. 7D). No binding of Arp2/3 to GST–SH2-Bβ beads was detected in either the absence or presence of ActA, with or without VASP (data not shown). In summary, the binding of SH2-Bβ to ActA is regulated by both VASP and the Arp2/3 complex, which are partners of ActA involved in the filament branching reaction. The data indicate that VASP strengthens the interaction of SH2-Bβ with ActA, whereas Arp2/3 weakens it.

Overall, the effects of SH2-Bβ on ActA-based motility and the binding data suggest that the regulated interaction between SH2-Bβ and ActA plays a role at the different elementary steps of the reaction of filament branching, thus modulating the catalytic efficiency.

DISCUSSION

In vivo and in vitro assays of actin-based motility of *Listeria* provide insight into the mechanism by which the adapter protein SH2-Bβ regulates actin-based motility. We found that SH2-Bβ stimulates actin-based propulsion of *Listeria* in vivo and in vitro and that removal of endogenous SH2-B inhibits actin-based propulsion of *Listeria*. This stimulatory effect of SH2-Bβ requires VASP, an activator of actin-based motility of *Listeria* that also stimulates motility of living cells by a mechanism that is still unclear. This result places SH2-Bβ on the same pathway as VASP in signaling to actin.

SH2-Bβ does not appear to bind VASP directly, but in the *Listeria* system it binds ActA, an effector of VASP, and the interaction between SH2-Bβ and ActA is enhanced by VASP. SH2-Bβ also binds F-actin in vitro, yet SH2-Bβ is detected specifically in highly motile ruffles and in *Listeria* actin tails in infected cells, while it is absent from stress fibers. The binding to F-actin measured in vitro, together with the selective localization of SH2-Bβ to those actin structures which are induced by filament branching in response to signaling, calls for an underlying molecular mechanism. Either the actin isoform composition of these structures, e.g., β-actin (15), promotes the selective binding of some regulatory proteins or subtle differences in the structure of actin filaments are induced by the different machineries that stimulate site-directed actin assembly by acting at barbed ends. Such differences might be used and amplified by specific regulators in a synergistic fashion. The fact that SH2-Bβ is found together with VASP on the surfaces of *Listeria* cells in newly formed short tails as well as along the long tails, away from VASP enrichment, suggests that SH2-Bβ may associate with the ActA-VASP complex at the surfaces of *Listeria* cells only temporarily, after which SH2-Bβ releases from the ActA-VASP complex and remains with actin as the tail elongates.

A higher level of regulation of *Listeria* movement is likely to exist in vivo than in vitro, since the effect of SH2-Bβ on *Listeria* motility is much greater in cells than in *Xenopus* egg extract and in reconstituted motility medium. This higher level of regulation is likely to require interaction of SH2-Bβ with a phosphotyrosine, an interaction shown previously to increase tyrosine and serine/threonine phosphorylation of SH2-Bβ (39), because SH2-Bβ with a defective SH2 domain acts as a dominant-negative mutant for *Listeria* motility in vivo. Although motile actin tails can be reconstituted using only five essential proteins, *Listeria* motility can be enhanced further by additional actin-regulating proteins present in *Listeria* tails in vivo (reviewed in reference 6); phosphorylation of SH2-Bβ may facilitate their recruitment. In support of this, SH2-Bβ(504-670) acts as a dominant-negative mutant in *Listeria* in cells but not in ActA-coated beads in motility medium, implicating amino acids 1 to 503 in maximal SH2-Bβ regulation of in vivo *Listeria* motility. This region of SH2-Bβ contains multiple post-translational modifications (29, 38), including at least one required for maximal in vivo SH2-Bβ enhancement of growth hormone-induced cell motility. Neither SH2-Bβ nor either of the above dominant-negative mutants of SH2-Bβ altered the number of *Listeria* cells with actin tails, indicating that the effect of SH2-Bβ is on tail length and motility rather than tail initiation. Thus, our findings do not conflict with previous results in which microinjection of an antiphosphotyrosine antibody into *Listeria*-infected cells failed to affect the ability of *Listeria* to induce actin tails (12).

Overexpression of SH2-Bβ enhances the motility of *Listeria* in cells only if VASP is present. The effect of SH2-Bβ is recapitulated not only in cell extracts but also in biomimetic motility assays of ActA-functionalized beads in the presence of only five proteins, and again VASP is required for the effect of SH2-Bβ. The latter observation restricts the number of mechanisms that can be invoked to account for the function of SH2-Bβ. The data strongly suggest that SH2-Bβ increases ActA-dependent motility only after prior recruitment of VASP to the surfaces of bacteria. VASP localizes in *Listeria* tails in MEF from SH2-$B^{-/-}$ as well as SH2-$B^{+/+}$ mice. In contrast, SH2-Bβ was not present in actin caps of ΔActA6 *Listeria* or in MV^{D7} cells lacking MENA/VASP, suggesting that VASP facilitates recruitment of SH2-Bβ to *Listeria*, thus allowing its association with actin in the tails. Quantitative motility measurements indicate that the effect of SH2-Bβ is most pronounced at low (e.g., 25 nM) concentrations of VASP, suggesting that SH2-Bβ strongly enhances the activity of VASP.

Binding studies bring some insight into the mechanism by which these mutual effects of VASP and SH2-Bβ develop. SH2-Bβ does not appear to interact with VASP directly; however, SH2-Bβ interacts with ActA, and its ability to interact with ActA is increased by VASP, consistent with the above in vivo data. In contrast, the ability of SH2-Bβ to bind to ActA is decreased by the Arp2/3 complex, which is the binding partner of ActA in filament branching. These facts raise the possibility that SH2-Bβ first binds to the ActA-VASP complex, enhancing the stability of this complex, and then dissociates from ActA upon binding of the Arp2/3 complex. We propose that the increased ability of SH2-Bβ to bind to ActA in the presence of VASP may be coupled to structural changes of ActA occurring during the catalytic cycle of filament branching, resulting in the faster release of the product of the reaction, i.e., the branched junction, in which both Arp2/3 and SH2-Bβ would be incorporated. In the branching catalytic cycle, SH2-Bβ would first bind ActA-VASP and then would dissociate from ActA and remain bound to F-actin.

The molecular mechanism by which VASP enhances motility is not fully understood (see reference 41 for a review). There is general agreement that VASP antagonizes the effect of capping proteins, thus promoting a decrease in the branching density in the dendritic actin array generated by filament branching with the Arp2/3 complex (3, 40), but whether VASP directly competes with capping proteins for barbed-end binding (1, 3) or acts indirectly to elicit this phenotype, e.g., by accelerating the rate-limiting step in filament branching (40), is not resolved. The fact that SH2-Bβ does not affect filament assembly, with or without VASP, but interacts transiently with ActA-VASP in the branching reaction suggests, but does not prove, that some modulation of the catalytic cycle of filament branching is at the origin of the effects of SH2-Bβ and VASP in motility.

ACKNOWLEDGMENTS

We are grateful to D. Portnoy (University of California at Berkeley, Berkeley, CA) and J. Theriot (Stanford University, Stanford, CA) for sending *Listeria* strains and for their very helpful advice. We thank M.

O'Riordan (University of Michigan) and J. Komarova (University of Michigan) for help with *Listeria* infection, L. Daniel (University of Michigan) for help with GST–SH2-Bβ purification, and B. Hawkins for assistance with the manuscript.

This work utilized the Morphology and Image Analysis Core of the Michigan Diabetes Research and Training Center, funded by grant NIH5P60 DK20572 from the National Institute of Diabetes and Digestive and Kidney Diseases. This work was supported by grants from the National Institutes of Health (R21-AI057778 [M.D.], R01-DK54222 [C.C.S.], R01-AI35950 [J.S.], RO1-DK065122 [L.Y.], and P60-DK20572 [MDRTC]), Deutsche Forschungsgemeinschaft (SFB 274 [C.K.]), Ligue Nationale Contre le Cancer (M.-F.C. is équipe labelisée Ligue 2003–2006), and the Human Frontier Science Program (RGP72/2003 [M.-F.C.]).

REFERENCES

1. **Barzik, M., T. I. Kotova, H. N. Higgs, L. Hazelwood, D. Hanein, F. B. Gertler, and D. A. Schafer.** 2005. Ena/VASP proteins enhance actin polymerization in the presence of barbed end capping proteins. J. Biol. Chem. **280:**28653–28662.
2. **Bear, J. E., J. J. Loureiro, I. Libova, R. Fassler, J. Wehland, and F. B. Gertler.** 2000. Negative regulation of fibroblast motility by Ena/VASP proteins. Cell **101:**717–728.
3. **Bear, J. E., T. M. Svitkina, M. Krause, D. A. Schafer, J. J. Loureiro, G. A. Strasser, I. V. Maly, O. Y. Chaga, J. A. Cooper, G. G. Borisy, and F. B. Gertler.** 2002. Antagonism between Ena/VASP proteins and actin filament capping regulates fibroblast motility. Cell **109:**509–521.
4. **Boujemaa-Paterski, R., E. Gouin, G. Hansen, S. Samarin, C. Le Clainche, D. Didry, P. Dehoux, P. Cossart, C. Kocks, M. F. Carlier, and D. Pantaloni.** 2001. Listeria protein ActA mimics WASp family proteins: it activates filament barbed end branching by Arp2/3 complex. Biochemistry **40:**11390–11404.
5. **Cicchetti, G., P. Maurer, P. Wagener, and C. Kocks.** 1999. Actin and phosphoinositide binding by the ActA protein of the bacterial pathogen Listeria monocytogenes. J. Biol. Chem. **274:**33616–33626.
6. **Cossart, P., and M. Lecuit.** 1998. Interactions of Listeria monocytogenes with mammalian cells during entry and actin-based movement: bacterial factors, cellular ligands and signaling. EMBO J. **17:**3797–3806.
7. **Diakonova, M., D. R. Gunter, J. Herrington, and C. Carter-Su.** 2002. SH2-Bbeta is a Rac-binding protein that regulates cell motility. J. Biol. Chem. **277:**10669–10677.
8. **Domann, E., J. Wehland, M. Rohde, S. Pistor, M. Hartl, W. Goebel, M. Leimeister-Wachter, M. Wuenscher, and T. Chakraborty.** 1992. A novel bacterial virulence gene in Listeria monocytogenes required for host cell microfilament interaction with homology to the proline-rich region of vinculin. EMBO J. **11:**1981–1990.
9. **Duan, C., M. Li, and L. Rui.** 2004. SH2-B promotes insulin receptor substrate 1 (IRS1)- and IRS2-mediated activation of the phosphatidylinositol 3-kinase pathway in response to leptin. J. Biol. Chem. **279:**43684–43691.
10. **Duan, C., H. Yang, M. F. White, and L. Rui.** 2004. Disruption of the SH2-B gene causes age-dependent insulin resistance and glucose intolerance. Mol. Cell. Biol. **24:**7435–7443.
11. **Egile, C., T. P. Loisel, V. Laurent, R. Li, D. Pantaloni, P. J. Sansonetti, and M. F. Carlier.** 1999. Activation of the CDC42 effector N-WASP by the Shigella flexneri IcsA protein promotes actin nucleation by Arp2/3 complex and bacterial actin-based motility. J. Cell Biol. **146:**1319–1332.
12. **Frischknecht, F., S. Cudmore, V. Moreau, I. Reckmann, S. Rottger, and M. Way.** 1999. Tyrosine phosphorylation is required for actin-based motility of vaccinia but not Listeria or Shigella. Curr. Biol. **9:**89–92.
13. **Geese, M., J. J. Loureiro, J. E. Bear, J. Wehland, F. B. Gertler, and A. S. Sechi.** 2002. Contribution of Ena/VASP proteins to intracellular motility of listeria requires phosphorylation and proline-rich core but not F-actin binding or multimerization. Mol. Biol. Cell **13:**2383–2396.
14. **Gertler, F. B., K. Niebuhr, M. Reinhard, J. Wehland, and P. Soriano.** 1996. Mena, a relative of VASP and Drosophila Enabled, is implicated in the control of microfilament dynamics. Cell **87:**227–239.
15. **Gunning, P., R. Weinberger, P. Jeffrey, and E. Hardeman.** 1998. Isoform sorting and the creation of intracellular compartments. Annu. Rev. Cell Dev. Biol. **14:**339–372.
16. **Haffner, C., T. Jarchau, M. Reinhard, J. Hoppe, S. M. Lohmann, and U. Walter.** 1995. Molecular cloning, structural analysis and functional expression of the proline-rich focal adhesion and microfilament-associated protein VASP. EMBO J. **14:**19–27.
17. **He, X., Y. Li, J. Schembri-King, S. Jakes, and J. Hayashi.** 2000. Identification of actin binding protein, ABP-280, as a binding partner of human Lnk adaptor protein. Mol. Immunol. **37:**603–612.
18. **Herrington, J., M. Diakonova, L. Rui, D. R. Gunter, and C. Carter-Su.** 2000. SH2-B is required for growth hormone-induced actin reorganization. J. Biol. Chem. **275:**13126–13133.
19. **Kocks, C., E. Gouin, M. Tabouret, P. Berche, H. Ohayon, and P. Cossart.** 1992. L. monocytogenes-induced actin assembly requires the actA gene product, a surface protein. Cell **68:**521–531.
20. **Kong, M., C. S. Wang, and D. J. Donoghue.** 2002. Interaction of fibroblast growth factor receptor 3 and the adapter protein SH2-B. A role in STAT5 activation. J. Biol. Chem. **277:**15962–15970.
21. **Kubo-Akashi, C., M. Iseki, S. M. Kwon, H. Takizawa, K. Takatsu, and S. Takaki.** 2004. Roles of a conserved family of adaptor proteins, Lnk, SH2-B, and APS, for mast cell development, growth, and functions: APS-deficiency causes augmented degranulation and reduced actin assembly. Biochem. Biophys. Res. Commun. **315:**356–362.
22. **Lanier, L. M., M. A. Gates, W. Witke, A. S. Menzies, A. M. Wehman, J. D. Macklis, D. Kwiatkowski, P. Soriano, and F. B. Gertler.** 1999. Mena is required for neurulation and commissure formation. Neuron **22:**313–325.
23. **Lasa, I., E. Gouin, M. Goethals, K. Vancompernolle, V. David, J. Vandekerckhove, and P. Cossart.** 1997. Identification of two regions in the N-terminal domain of ActA involved in the actin comet tail formation by Listeria monocytogenes. EMBO J. **16:**1531–1540.
24. **Laurent, V., T. P. Loisel, B. Harbeck, A. Wehman, L. Grobe, B. M. Jockusch, J. Wehland, F. B. Gertler, and M. F. Carlier.** 1999. Role of proteins of the Ena/VASP family in actin-based motility of Listeria monocytogenes. J. Cell Biol. **144:**1245–1258.
25. **Loisel, T. P., R. Boujemaa, D. Pantaloni, and M. F. Carlier.** 1999. Reconstitution of actin-based motility of Listeria and Shigella using pure proteins. Nature **401:**613–616.
26. **Machner, M. P., C. Urbanke, M. Barzik, S. Otten, A. S. Sechi, J. Wehland, and D. W. Heinz.** 2001. ActA from Listeria monocytogenes can interact with up to four Ena/VASP homology 1 domains simultaneously. J. Biol. Chem. **276:**40096–40103.
27. **Mounier, J., A. Ryter, M. Coquis-Rondon, and P. J. Sansonetti.** 1990. Intracellular and cell-to-cell spread of *Listeria monocytogenes* involves interaction with F-actin in the enterocyte-like cell line Caco-2. Infect. Immun. **58:**1048–1058.
28. **Niebuhr, K., F. Ebel, R. Frank, M. Reinhard, E. Domann, U. D. Carl, U. Walter, F. B. Gertler, J. Wehland, and T. Chakraborty.** 1997. A novel proline-rich motif present in ActA of Listeria monocytogenes and cytoskeletal proteins is the ligand for the EVH1 domain, a protein module present in the Ena/VASP family. EMBO J. **16:**5433–5444.
29. **O'Brien, K. B., L. S. Argetsinger, M. Diakonova, and C. Carter-Su.** 2003. YXXL motifs in SH2-Bbeta are phosphorylated by JAK2, JAK1, and platelet-derived growth factor receptor and are required for membrane ruffling. J. Biol. Chem. **278:**11970–11978.
30. **Pantaloni, D., and M. F. Carlier.** 1993. How profilin promotes actin filament assembly in the presence of thymosin beta 4. Cell **75:**1007–1014.
31. **Pantaloni, D., C. Le Clainche, and M. F. Carlier.** 2001. Mechanism of actin-based motility. Science **292:**1502–1506.
32. **Pistor, S., L. Grobe, A. S. Sechi, E. Domann, B. Gerstel, L. M. Machesky, T. Chakraborty, and J. Wehland.** 2000. Mutations of arginine residues within the 146-KKRRK-150 motif of the ActA protein of Listeria monocytogenes abolish intracellular motility by interfering with the recruitment of the Arp2/3 complex. J. Cell Sci. **113:**3277–3287.
33. **Qian, X., A. Riccio, Y. Zhang, and D. D. Ginty.** 1998. Identification and characterization of novel substrates of Trk receptors in developing neurons. Neuron **21:**1017–1029.
34. **Reinhard, M., M. Halbrugge, U. Scheer, C. Wiegand, B. M. Jockusch, and U. Walter.** 1992. The 46/50 kDa phosphoprotein VASP purified from human platelets is a novel protein associated with actin filaments and focal contacts. EMBO J. **11:**2063–2070.
35. **Rottner, K., B. Behrendt, J. V. Small, and J. Wehland.** 1999. VASP dynamics during lamellipodia protrusion. Nat. Cell Biol. **1:**321–322.
36. **Rui, L., and C. Carter-Su.** 1999. Identification of SH2-bbeta as a potent cytoplasmic activator of the tyrosine kinase Janus kinase 2. Proc. Natl. Acad. Sci. USA **96:**7172–7177.
37. **Rui, L., D. R. Gunter, J. Herrington, and C. Carter-Su.** 2000. Differential binding to and regulation of JAK2 by the SH2 domain and N-terminal region of SH2-bbeta. Mol. Cell. Biol. **20:**3168–3177.
38. **Rui, L., J. Herrington, and C. Carter-Su.** 1999. SH2-B, a membrane-associated adapter, is phosphorylated on multiple serines/threonines in response to nerve growth factor by kinases within the MEK/ERK cascade. J. Biol. Chem. **274:**26485–26492.
39. **Rui, L., L. S. Mathews, K. Hotta, T. A. Gustafson, and C. Carter-Su.** 1997. Identification of SH2-Bbeta as a substrate of the tyrosine kinase JAK2 involved in growth hormone signaling. Mol. Cell. Biol. **17:**6633–6644.
40. **Samarin, S., S. Romero, C. Kocks, D. Didry, D. Pantaloni, and M. F. Carlier.** 2003. How VASP enhances actin-based motility. J. Cell Biol. **163:**131–142.
41. **Sechi, A. S., and J. Wehland.** 2004. ENA/VASP proteins: multifunctional regulators of actin cytoskeleton dynamics. Front. Biosci. **9:**1294–1310.
42. **Skoble, J., D. A. Portnoy, and M. D. Welch.** 2000. Three regions within ActA promote Arp2/3 complex-mediated actin nucleation and Listeria monocytogenes motility. J. Cell Biol. **150:**527–538.
43. **Smith, G. A., J. A. Theriot, and D. A. Portnoy.** 1996. The tandem repeat domain in the Listeria monocytogenes ActA protein controls the rate of actin-based motility, the percentage of moving bacteria, and the localization

of vasodilator-stimulated phosphoprotein and profilin. J. Cell Biol. **135:**647–660.
44. **Spudich, J. A., and S. Watt.** 1971. The regulation of rabbit skeletal muscle contraction. I. Biochemical studies of the interaction of the tropomyosin-troponin complex with actin and the proteolytic fragments of myosin. J. Biol. Chem. **246:**4866–4871.
45. **Theriot, J. A., T. J. Mitchison, L. G. Tilney, and D. A. Portnoy.** 1992. The rate of actin-based motility of intracellular Listeria monocytogenes equals the rate of actin polymerization. Nature **357:**257–260.
46. **Theriot, J. A., J. Rosenblatt, D. A. Portnoy, P. J. Goldschmidt-Clermont, and T. J. Mitchison.** 1994. Involvement of profilin in the actin-based motility of L. monocytogenes in cells and in cell-free extracts. Cell **76:**505–517.
47. **Tilney, L. G., and D. A. Portnoy.** 1989. Actin filaments and the growth, movement, and spread of the intracellular bacterial parasite, Listeria monocytogenes. J. Cell Biol. **109:**1597–1608.
48. **Wang, J., and H. Riedel.** 1998. Insulin-like growth factor-I receptor and insulin receptor association with a Src homology-2 domain-containing putative adapter. J. Biol. Chem. **273:**3136–3139.
49. **Welch, M. D., A. Iwamatsu, and T. J. Mitchison.** 1997. Actin polymerization is induced by Arp2/3 protein complex at the surface of Listeria monocytogenes. Nature **385:**265–269.
50. **Welch, M. D., and R. D. Mullins.** 2002. Cellular control of actin nucleation. Annu. Rev. Cell Dev. Biol. **18:**247–288.
51. **Welch, M. D., J. Rosenblatt, J. Skoble, D. A. Portnoy, and T. J. Mitchison.** 1998. Interaction of human Arp2/3 complex and the Listeria monocytogenes ActA protein in actin filament nucleation. Science **281:**105–108.
52. **Wiesner, S., E. Helfer, D. Didry, G. Ducouret, F. Lafuma, M. F. Carlier, and D. Pantaloni.** 2003. A biomimetic motility assay provides insight into the mechanism of actin-based motility. J. Cell Biol. **160:**387–398.

Editor: J. B. Bliska